frontiers | Frontiers in Mechanical Engineering

TYPE Original Research
PUBLISHED 14 May 2025
DOI 10.3389/fmech.2025.1531864

OPEN ACCESS

EDITED BY
Snehal Shetye,
United States Food and Drug Administration, United States

REVIEWED BY
Federica Buccino,
Fondazione Politecnico di Milano, Italy
Mengcun Chen,
University of Pennsylvania, United States

*CORRESPONDENCE
Octavio A. González-Estrada,
agonzale@uis.edu.co

RECEIVED 21 November 2024
ACCEPTED 30 April 2025
PUBLISHED 14 May 2025

CITATION
Castillo F, Hernández-Salazar CA and González-Estrada OA (2025) Structural analysis of the hip joint using segmentation and finite elements in patients with femoroacetabular impingement.
Front. Mech. Eng. 11:1531864.
doi: 10.3389/fmech.2025.1531864

Structural analysis of the hip joint using segmentation and finite elements in patients with femoroacetabular impingement

Felipe Castillo, Cristian A. Hernández-Salazar and Octavio A. González-Estrada *

School of Mechanical Engineering, Universidad Industrial de Santander, Bucaramanga, Colombia

Musculoskeletal disorders pose a significant challenge due to their profound impact on mobility and quality of life. Among these, cam-type femoroacetabular impingement stands out for its effect on femoral head morphology, causing joint pain and limiting movement. This study explores the biomechanical consequences of cam-type impingement through comprehensive analysis using computed tomography (CT) scans. Advanced 3D segmentation performed with 3D Slicer software enabled precise three-dimensional hip joint models. Mechanical properties, including Young's modulus and density, were directly derived from CT data and integrated into finite element models developed in Ansys. The simulations assessed the hip joint's response during flexion and abduction, replicating dynamic conditions commonly encountered in daily activities. Results demonstrated that cam-type impingement leads to elevated stress concentrations and altered contact patterns. Abduction generated the highest strain values, reaching 0.0578 mm/mm, while flexion induced greater relative changes, with up to a 22.72% variation between healthy and affected joints. These findings provide critical insights into joint mechanics under pathological conditions, underscoring the potential of biomechanical modeling for enhancing diagnostic accuracy and therapeutic interventions. By identifying stress concentration zones, the study highlights the utility of finite element models in designing improved surgical techniques and targeted rehabilitation protocols, ultimately advancing treatment outcomes for patients with femoroacetabular impingement.

KEYWORDS

3D segmentation, femoroacetabular impingement, hip joint mechanics, finite element analysis, patient-specific modeling

1 Introduction

Due to their profound influence on healthcare systems and the quality of life of individuals, musculoskeletal disorders have emerged as a crucial area of research (Shapiro, 2021). These conditions have been diagnosed in an estimated 120 million adults, exceeding the prevalence of other diseases like hypertension and asthma (Shapiro, 2021). It's noteworthy that these diseases have been diagnosed in a significant proportion of the population, with about 47% of men and 53% of women affected (Shapiro, 2021). These conditions are primarily linked to joint injuries or disorders that hinder free movement, impacting not just the muscles but also the skeletal system that supports and safeguards the

soft tissues (Lafita, 2003). Consequently, the skeletal system can lose these properties due to a multitude of diseases, including osteoporosis, cam-type femoroacetabular impingement, and osteoarthritis, which degrade the patient's quality of life (Jiménez and Cuenca, 2015; Rachner et al., 2011; Morgado et al., 2005).

Medical imaging techniques such as X-rays, (Liberman et al., 1995), computed tomography (CT) (Scranton et al., 2000), and magnetic resonance imaging are frequently employed to diagnose damage in bone structures (Myers et al., 1999). The field of radiomics has brought about a revolution in CT scans, enabling the generation of 3D models from precise segmentations. These methods dissect the images and extract pertinent sections for in-depth analysis, paving the way for new opportunities in the study and comprehension of anatomical structures and diseases (Garcia and Nicot, 2007). Software like 3D Slicer (Fedorov et al., 2012), In Vesalius (Camilo et al., 2012), and ITK Snap (Yushkevich et al., 2006), are popular for image segmentation. Technological advancements have made it feasible to create controlled environments for simulating scenarios involving loads and deformations in joint movements. (Longo et al., 2021). The finite element method has gained widespread acceptance in medical research due to its crucial role in conducting precise and realistic models (Mejía Rodríguez et al., 2024)– (Maldonado-Moreno et al., 2024). This technique offers invaluable insights into biomechanics, enhancing our understanding of structural behavior and fostering the creation of innovative solutions (Ardila Parra et al., 2019), (Zhang et al., 2022).

The presence of hip pain is a condition that affects many young people worldwide. However, its prevalence has been observed to be higher in certain groups, such as high-performance athletes, particularly professional footballers, where it can affect up to 18% of the population (Maldonado et al., 2023), (Kemp et al., 2020). The hip joint is an essential structure for the performance of daily activities in people. This joint is composed of the femoral head and the acetabulum, which connect the trunk with the lower extremities (Navarro-Zarza et al., 2012), (Noble et al., 2017). Due to the variations of movement that occur in the joint area, a large number of diseases that affect movement can occur, among which is femoroacetabular impingement (FAI), which generates a structural abnormality that results in direct contact between the femur and the acetabulum (Camacho and Mardones, 2013). Variations of this disease include cam-type impingement and pincer-type impingement, which are differentiated according to the area that is affected In cam impingement, a deformity is generated in the femur so that shear forces develop in the acetabular cartilage, and for pincer impingement, a variation in the acetabulum is present, resulting in increased stress on the femoral head (Sarassa et al., 2021).

In recent years, studies have used modeling tools to obtain 3D models and evaluate stresses in body biomechanics during different activities (Grubor et al., 2019; Yong et al., 2018; Souza and Naves, 2019). For example, in the study (Ng et al., 2012), changes in stress concentrations in the anterosuperior zone of the bone during squats were evaluated, finding an average change of 15.2 ± 1.8 MPa. Similarly, virtual models have been employed to determine the ideal extent of osteoplasty required for reducing femoroacetabular contact. These methodologies underscore the potential of such processes to evolve into future tools, given their strong resemblance to conventional calculations conducted by medical professionals. This advancement paves the way for virtual technology to enhance traditional diagnostic and treatment approaches (Bagce et al., 2021). Other observational studies detailed the ranges of motion (flexion, internal and external rotation) finding relationships between impingement and posterior femoroacetabular impingement, so that contact between the acetabulum and femoral neck is related to the symptomatology of anterior femoroacetabular impingement (AFAI) (Aguilera et al., 2020). Similarly, the use of finite element analysis has allowed the study of alterations in the hip joint due to impingement, which leads to an increase in intrinsic pressure, resulting in joint wear, in addition to an influence on the cartilaginous tissues (Hellwig et al., 2016). The evaluation of the movements allowed by the hip joint, such as flexion, evidences how the change in angle of this movement generates an increase in the contact pressure of the area, having changes from 8.2 MPa to 13.3 MPa in only 45 degrees of difference (Jorge et al., 2014). Additionally, this study (Hernández-Salazar et al., 2024), demonstrates how experimental tests and finite element analysis can provide valuable insights into bone behavior and guide the design of safer and effective medical implants.

FAI is classified into two main types: cam-type and pincer-type. Cam-type FAI is characterized by an abnormal femoral head morphology that induces high shear stresses on the acetabular cartilage. This work analyzes its effects using CT-based segmentation to create 3D models of the hip joint. By incorporating anisotropic properties into the finite element models, the research evaluates stress and strain variations during flexion and abduction movements, providing a comprehensive understanding of the mechanical behavior of affected joints and contributing to the development of targeted treatments that improve clinical outcomes.

2 Materials and methods

The implementation of the structural analysis of the hip joint was carried out in three distinct stages: the review of CT scans, the identification of the mechanical properties of the bone, and the development of a finite element model to simulate contact. These steps facilitated obtaining three-dimensional representations of the patients, identified crucial aspects of bone behavior, and established the conditions for the simulation, including allowable flexion and abduction motions in the hip region.

2.1 CT analysis and model segmentation from medical image

In the initial phase of this study, computed axial tomography scans of patients with cam-type FAI were meticulously examined to identify structural irregularities, as depicted in Figure 1. The medical images, which were anonymized, were provided by 3D Medical Innovation SAS. These images were captured using a Philips CT scanner, featuring a matrix size of 410 × 410, a window width of 157, a pixel pitch of 0.28 mm, and a slice pitch of 4 mm.

Based on the model review and selection process described above, segmentation was performed using the open-source

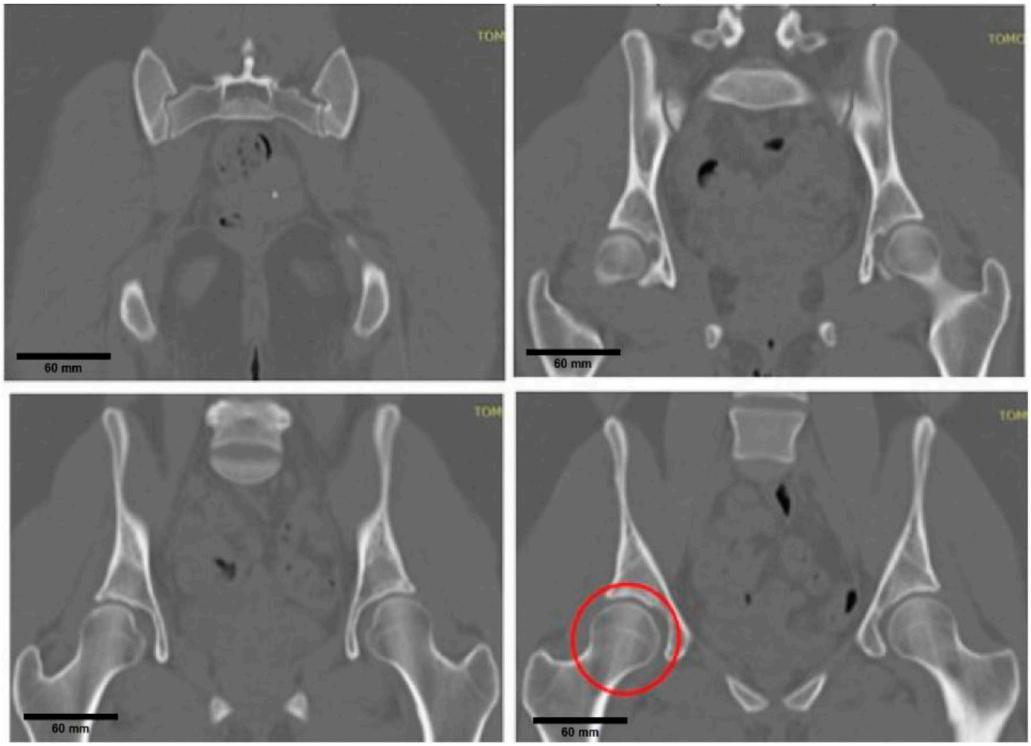

FIGURE 1
Medical imaging review process, highlighting cam-type femoroacetabular impingement.

software 3D Slicer, designed to work with CT scans. In this software, the Threshold tool was used to identify areas of interest related to the hip joint, assigning them a distinctive green color, as shown in Figure 2.

2.2 Bone properties

To assign the characteristic properties of bone, including density and elastic modulus, Bonemat software (Pegg and Gill, 2016) was utilized. We evaluate bone properties based on Equations 1, 2 derived from Hounsfield Unit (HU) values. These equations, originally developed from our experimental work and implemented in (Hernández-Salazar et al., 2024), define the bone density ρ as follows:

$$\rho = -3.210e13 + 1.00e11HU \tag{1}$$

From this density equation, the elastic modulus E is determined using:

$$E = 1.8e10 + 2.20e6\rho \tag{2}$$

These relationships ensure that the material properties assigned in the finite element analysis accurately reflect the non-homogeneous nature of bone tissue. Figure 3 shows how two nearby points can exhibit different values. To account for this

FIGURE 2
In joint segmentation, the detailed green color is attributed to the bone of interest to generate the three-dimensional model.

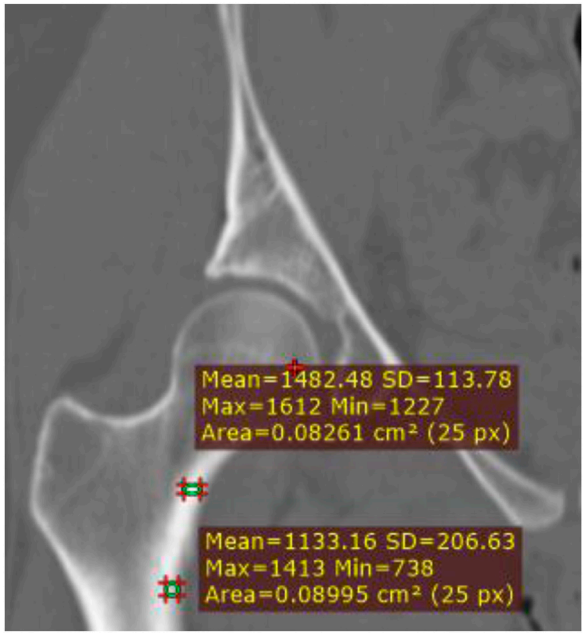

FIGURE 3
Variations in Hounsfield Units (HU) within bone tissue.

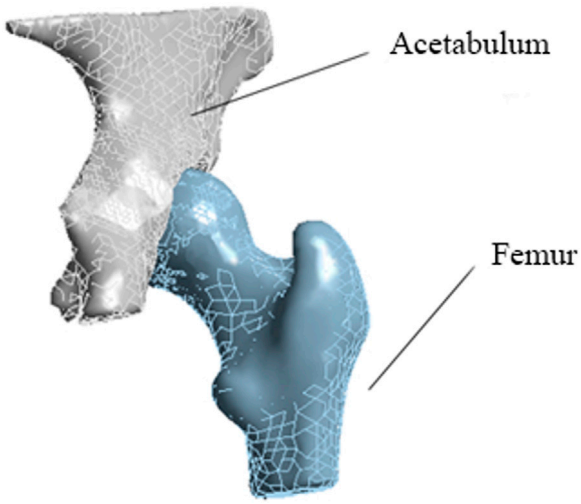

FIGURE 4
Meshed femur and acetabulum models. The mesh consists of quadratic tetrahedral elements to capture the structural behavior of the hip joint accurately.

variability, a linear interpolation method was applied, enabling the determination of Young's modulus, density, and Hounsfield Units (HU) based on their location in the CT scan, with ranges of 15–20 GPa for Young's modulus, 0.97–1.73 g/cm^3 for density, and 300–600 for HU. Poisson's ratio was fixed at 0.3 throughout the analysis.

2.3 Finite element model

The finite element method was used to represent the structural model and simulate its elastic behavior. From the STL models obtained from the study patient, the meshes of the hip joints were created using Ansys software, and a characteristic mesh of 172325 nodes and 120256 quadratic tetrahedron elements were formed, as shown in Figure 4.

A mesh independence test was performed to establish the mesh, as illustrated in Table 1. Three different resolutions, each with a different number of elements and nodes, were used to evaluate the consistency of the displacement results with increasing mesh resolution. The findings suggest that, by increasing the number of nodes and elements, the accuracy of the results is maintained with a reduced percentage error, indicating adequate mesh independence with a higher number of nodes and elements.

The constraints applied to the models simulate dynamic conditions, particularly focusing on the abduction and flexion movements of the hip joint, as illustrated in Figure 5. In Figure 5a, the simulation represents the abduction movement, where the angle between the femur and pelvis changes due to lateral movement of the leg. This movement affects the stress distribution across the femoral head and acetabulum. Meanwhile, Figure 5b shows the flexion movement, where the femur moves forward relative to the pelvis, creating different stress patterns in the joint. These models allow the identification of changes in bone loading by varying the angle and corresponding activity in the femoracetabular joint.

Under normal conditions, the hip joint allows a range of motion of 120°–140° in flexion, 40°–50° in abduction, and 30°–50° in internal-external rotation. However, in cam-type FAI, this range is often restricted due to abnormal contact between the femoral head and the acetabulum, leading to increased stress concentration. To analyze this, our simulations focused on flexion and abduction at 3°, 7°, and 15°, representing limited joint mobility.

To simulate the mechanical behavior of the bone in the hip joint, dynamic conditions are imposed on the models. This allows the femur to rotate within the acetabulum, mimicking the natural motion of the hip. Concurrently, the acetabulum remains static, while the femur is permitted to move through three pre-established angles, as depicted in Figure 6a. A frictionless contact was established between the two bodies with a pinball radius of 10 mm, and a simulation time with sub steps ranging from a minimum of 7 to a maximum of 50 was utilized. Lastly, a load was applied to the underside of the femoral head to simulate the patient's weight, as illustrated in Figure 6b.

3 Results and discussion

3.1 Comparison of movements

Through the process of motion simulation, we assessed two types of activities in two distinct models: one representing healthy condition and the other depicting cam-type impingement. The results obtained for bending, which include the stresses and strains developed across three different angles, are presented in Table 2.

Table 2 shows a greater increase in stresses in the model with cam-type impingement, due to the excess bone that develops in the

TABLE 1 Mesh independence.

Resolution	Nodes	Elements	Displacement (mm)	% error
2	68540	54320	1.211	5.6
3	102896	90623	1.145	0.17
4	172325	120256	1.147	-

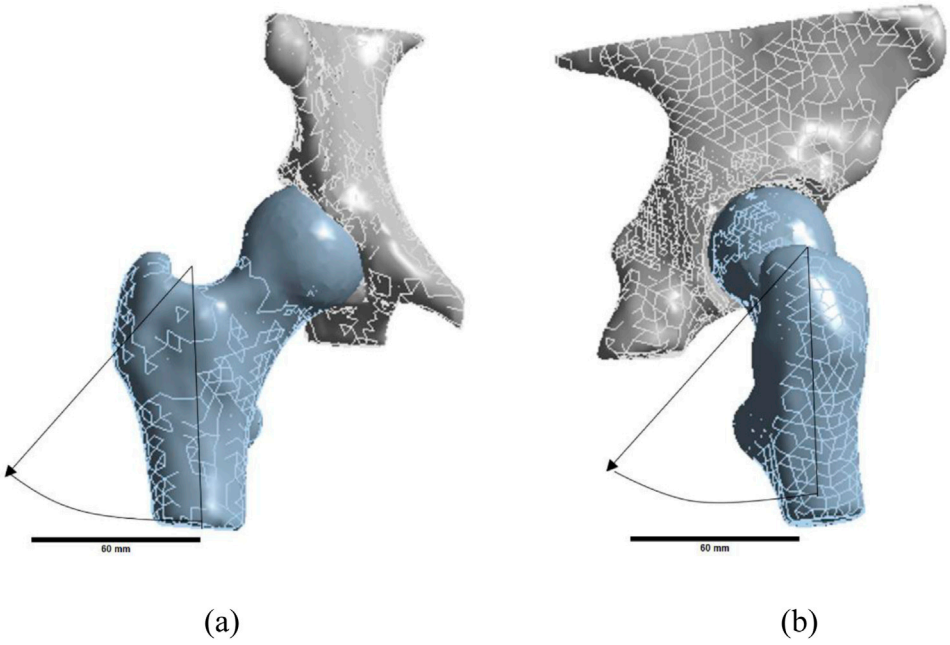

FIGURE 5
Permitted movements: **(a)** abduction and **(b)** flexion. These movements represent the primary dynamic conditions evaluated in the finite element analysis.

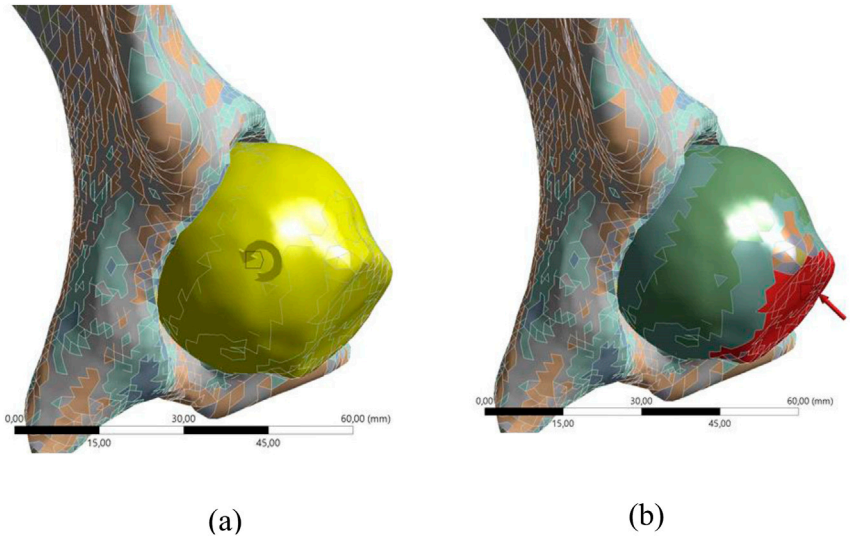

FIGURE 6
Boundary conditions: **(a)** shows the femur's motion within the acetabulum under dynamic conditions, and **(b)** illustrates the applied load to simulate the patient's body weight on the femoral head.

TABLE 2 Results in bending movements. The strain values obtained for different bending angles in both healthy and cam-type FAI models. The percentage difference highlights the increased strain experienced in impinged joints, which may contribute to joint degeneration and altered biomechanics.

Angle (°)	Difference (%)	Strain, cam-type (mm/mm)	Strain, healthy (mm/mm)	Difference (%)
3	11.72	0.01167	0.01059	10.19
7	22.12	0.02824	0.02447	15.40
15	13.25	0.06024	0.05921	1.74

TABLE 3 Abduction results. Strain values for different abduction angles in healthy and cam-type FAI models. The percentage difference quantifies the increased strain in the impinged joint, revealing higher stress concentrations compared to the healthy model.

Angle (°)	Difference (%)	Strain, cam-type (mm/mm)	Strain, healthy (mm/mm)	Difference (%)
3	9.058	0.0116	0.0107	8.78
7	16.09	0.0273	0.0237	15.18
15	13.65	0.0578	0.0491	17.71

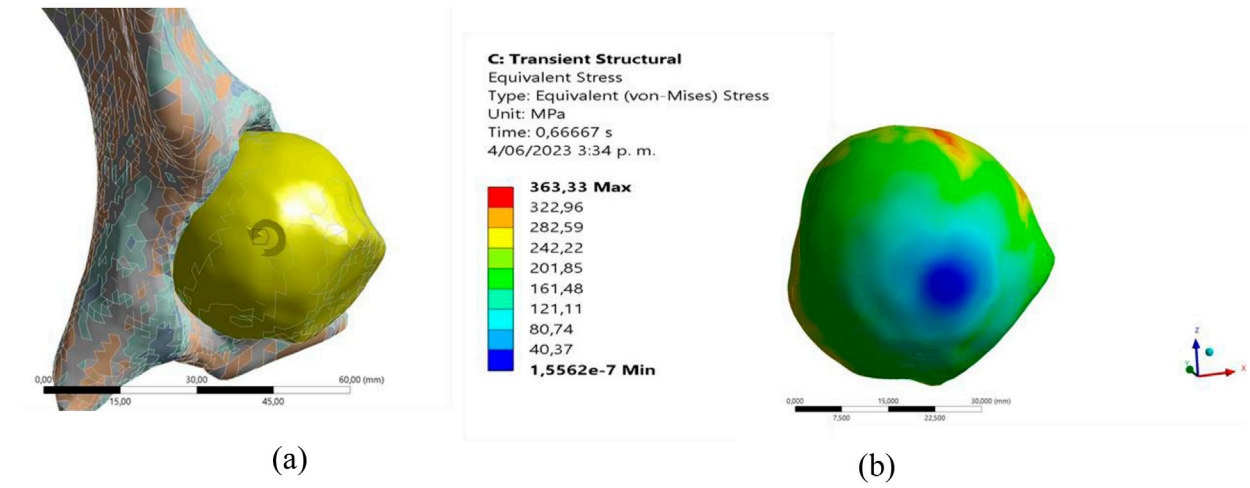

FIGURE 7
Maximum forces in the contact zone in abduction: **(a)** femur movement, **(b)** stress distribution.

femoral head because of the disease. In addition, it is observed how the angle increases affect the stresses and deformations, highlighting a proportional behavior as the evaluated angle increases. However, a greater proportional difference between the values of the healthy bone and the cam type for a specific angle, as is the case of 7°, is appreciated. In the second motion analysis, abduction was evaluated, with the results presented in Table 3.

As in the bending analysis, a trend is observed in the influence of the angle evaluated on the stresses and deformations. However, it was found that, in this case, the movement performed also influences the stress increases, and a higher increase is observed compared to bending.

3.2 Contact problem

Finite element analysis was used to evaluate the contact between the surfaces of the acetabulum and femur. Figure 7 shows how stress is concentrated in the lateral area of the femur during the abduction movement when contact between these two surfaces occurs.

It is important to note that the point of concentration varies according to the type of movement, as can be seen in Figure 8. When evaluating the flexion movement, a change in the position of concentration is evident in comparison with abduction, presenting a greater concentration in the frontal area of the femur.

Comparing stress distribution in cam-type FAI across different studies reveals notable differences in how joint mechanics are modeled. Previous research (Jorge et al., 2014), has analyzed stress variations in affected hip joints, but the relative percentage differences observed in our study highlight the impact of joint movement on stress distribution. Flexion results in a greater relative change (up to 22% difference between healthy and affected joints), while abduction consistently shows higher stress concentration values. The consistency of these results with established literature supports the reliability of the finite element

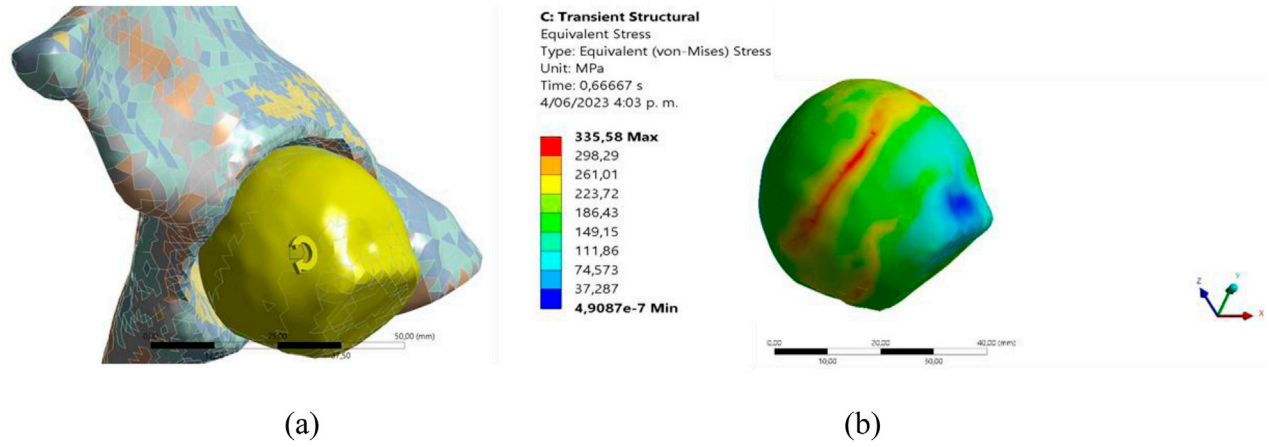

FIGURE 8
Maximum stress in the contact zone in bending: **(a)** motion model, **(b)** stress distribution.

model. Additionally, the bone material properties used in this study were assigned following well-documented density-modulus relationships derived from CT data (Hernández-Salazar et al., 2024; Pegg and Gill, 2016), which have been validated in experimental studies. While direct validation against vitro or *in vivo* data was not performed, the observed trends align with previous computational and experimental investigations in hip biomechanics. Future work will incorporate subject-specific gait analysis or cadaveric experiments to further validate the findings and enhance clinical applicability.

While the finite element model effectively captures stress distribution in the hip joint, the exclusion of soft tissues, such as cartilage, ligaments, and muscles, introduces certain limitations in the mechanical response representation. Excluding these components isolates the direct bone-to-bone interaction in cam-type femoroacetabular impingement, allowing a focused analysis of stress distribution in bony structures. Similar methodologies have been used in previous finite element studies (Jorge et al., 2014; Lostado Lorza et al., 2021) to evaluate the mechanical response of the hip joint. However, the absence of cartilage likely overestimates localized stress concentrations, as cartilage distributes loads and reduces peak stresses. Ligaments and muscles also influence joint stability and force transmission, affecting strain patterns and displacement characteristics. Future work will integrate these components using hyperelastic or viscoelastic material models to enhance the physiological accuracy and clinical applicability of the simulations.

A more detailed comparison with existing literature reveals that previous studies on hip joint biomechanics have employed both rigid and deformable models to evaluate stress distribution in cam-type femoroacetabular impingement. In studies such as (Ng et al., 2012) and (Hellwig et al., 2016), finite element models included cartilage layers, which led to lower peak stress values due to their cushioning effect. In contrast, the present study models direct bone-to-bone contact, resulting in higher stress concentrations in the femoral head and acetabulum. Additionally, prior research (Jorge et al., 2014; Lostado Lorza et al., 2021) has mainly focused on static loading conditions, whereas this study incorporates dynamic flexion and abduction movements, providing a more physiologically relevant assessment of joint mechanics. The results indicate that abduction produces the highest strain values (0.0578 mm/mm), consistent with the findings of (Jorge et al., 2014), but also show a more pronounced percentage variation in flexion, highlighting the impact of movement-specific loading conditions. These insights contribute to the broader understanding of hip joint biomechanics by demonstrating the importance of patient-specific modeling and dynamic simulations in assessing joint stress distributions.

Due to the concentration points generated, displacements across various evaluated angles are noted. As depicted in Table 4, the results of the abduction movement are presented, underscoring a more significant impact in instances of cam-type impingement.

Table 5 presents the results of the flexion movement, which indicate that the influence of impingement is maintained. However, it is important to note that, in both cases, the abduction movement continues to be the main generator of displacements.

The results obtained in this work present a great difference with respect to (Lostado Lorza et al., 2021) due to the exposure conditions of the bone. In our study, there was a contact between two materials with similar properties and strengths, which resulted in higher stresses compared to (Lostado Lorza et al., 2021), where a contact between bone and acetabular cartilage was presented being this a material with lower properties and less resistant. Despite these differences, the trend of the results was maintained, where greater stress was observed when the femur had cam-type impingement.

The accuracy of finite element simulations depends significantly on the choice of input parameters, including material properties, boundary conditions, and mesh resolution (Mejía Rodríguez et al., 2024; Cheng et al., 2016; Grubor et al., 2019). In this study, material properties were derived using established density-modulus relationships (Pegg and Gill, 2016), ensuring consistency with previously reported experimental data (Hernández-Salazar et al., 2024). Boundary conditions were set to replicate physiological loading scenarios observed in hip joint mechanics (Longo et al., 2021; Navarro-Zarza et al., 2012). Mesh sensitivity analysis was conducted to confirm result stability, demonstrating that finer meshes did not significantly alter stress distributions (Ng et al., 2012; Hernández-Salazar et al., 2024). While the selected parameters align with established methodologies, their influence on the outcomes must be considered.

TABLE 4 Results of abduction displacements. Displays displacement values for different abduction angles in healthy and cam-type FAI models. The percentage difference highlights the increased displacement in the impinged joint, indicating altered joint mechanics and potential mobility restrictions.

Angle (°)	Displacement, cam-type (mm)	Displacement, healthy (mm)	Difference (%)
3	1.255	1.099	14.19
7	2.836	2.239	26.6
15	5.985	5.366	11.53

TABLE 5 Results of bending displacements. Displays displacement values for different bending angles in healthy and cam-type FAI models.

Angle (°)	Displacement, cam-type (mm)	Displacement, healthy (mm)	Difference (%)
3	1.147	1.025	11.9
7	2.679	2.183	22.72
15	5.786	5.191	11.46

Excluding soft tissues such as cartilage, ligaments, and muscles isolates the direct bone-to-bone interaction in cam-type femoroacetabular impingement, allowing a focused analysis of stress distribution in bony structures. Similar methodologies have been used in previous finite element studies ((Jorge et al., 2014), (Lostado Lorza et al., 2021)) to evaluate the mechanical response of the hip joint. However, the absence of cartilage likely overestimates localized stress concentrations, as cartilage distributes loads and reduces peak stresses. Ligaments and muscles also influence joint stability and force transmission, affecting strain patterns and displacement characteristics. Future work will integrate these components using hyperelastic or viscoelastic material models to enhance the physiological accuracy and clinical applicability of the simulations.

4 Conclusion

The findings from this study underscore the biomechanical impact of cam-type FAI on joint strain distribution and mobility. Using advanced segmentation and finite element analysis, we demonstrated that cam-type impingement significantly increases strain concentrations in the femoral head, with abduction reaching strain values up to 0.0578 mm/mm. Flexion movements, while generating lower absolute strain levels, exhibited a greater percentage variation (22.72%) compared to healthy joints, highlighting their pronounced influence on joint mechanics. These results reveal that both movements—flexion and abduction—have distinct and critical effects on strain distribution and deformation in impinged joints.

This research contributes significantly to biomechanical studies by offering detailed insights into how joint contacts evolve during specific hip movements affected by FAI. By precisely identifying stress concentration zones, the study provides a robust framework for enhancing the diagnosis and treatment of hip disorders. The integration of segmentation and FEA methods not only advances the understanding of joint mechanics but also bridges the gap between theoretical models and clinical applications.

From a clinical perspective, these findings have direct implications for improving surgical interventions, such as osteoplasty, by identifying the most affected zones requiring correction. Additionally, the results support the optimization of rehabilitation protocols, enabling the design of personalized exercises to minimize joint stress and prevent further damage. This is particularly relevant for athletes and individuals engaged in high-impact activities, where targeted prevention strategies could significantly reduce the risk of joint degeneration.

Beyond the immediate applications, this work highlights the potential for using patient-specific biomechanical models in developing custom prosthetics and implants. As demonstrated here, these models ensure a more accurate representation of individual variations by incorporating anisotropic bone properties, paving the way for safer and more effective orthopedic solutions. These insights into the dynamic behavior of hip joints under pathological conditions also contribute to the broader field of musculoskeletal research, providing a foundation for further exploration of other joint disorders and their biomechanical implications.

The models used in this study were based solely on computed tomography (CT) scans, which are highly effective for bone segmentation but do not account for soft tissues such as cartilage, ligaments, and muscles. These tissues are essential in joint mechanics, and their exclusion may influence the accuracy of stress and displacement predictions. Additionally, the finite element analysis employed static boundary conditions and assumed frictionless contact between the femoral head and acetabulum. While these simplifications improve computational efficiency, they do not fully replicate the complexities of real-life dynamic interactions within the joint. The material properties assigned to the bone were derived from Hounsfield units (HU) using a linear interpolation approach. Although effective for this type of analysis, this method does not consider potential nonlinearities in bone behavior, particularly under extreme loading scenarios. Moreover, the study focused exclusively on cam-type FAI, leaving pincer-type and mixed forms of the condition unexplored, even though these variants might exhibit distinct biomechanical behaviors. The sample size was limited, potentially restricting the generalizability of the findings to broader patient populations with different anatomical and pathological characteristics. Addressing these considerations in future research will enhance the robustness of the models, their clinical relevance, and their ability to guide personalized treatment planning.

While this study provides valuable insights into the biomechanical effects of cam-type femoroacetabular

impingement, certain simplifications were necessary to maintain computational feasibility. The exclusive focus on cam-type FAI was driven by its high prevalence and impact on early hip degeneration, while including pincer-type and mixed variants would require different modeling approaches. Similarly, the use of static boundary conditions and frictionless contact simplifies joint mechanics but does not fully capture dynamic interactions. Future research will incorporate dynamic loading conditions and frictional effects to improve model accuracy. Additionally, while linear interpolation was used to assign bone material properties, this approach may not fully reflect non-linear effects under high loads. Future research could refine material modeling to better represent bone response under extreme stress, further enhancing the predictive capabilities of finite element analysis and providing a more realistic simulation of biomechanical behavior.

Moreover, future studies should consider integrating soft tissues, such as cartilage, ligaments, and muscles, into biomechanical models to provide a more holistic understanding of joint mechanics. Incorporating dynamic boundary conditions and frictional contact in finite element simulations would improve the accuracy and clinical relevance of the analyses. Expanding the scope to include pincer-type and mixed forms of cam-type FAI would also enhance the applicability of the findings, as these variants may present unique biomechanical challenges. Additionally, advancements in material modeling should focus on incorporating nonlinear properties and anisotropic behaviors to refine stress and strain predictions, especially under extreme loading conditions. Increasing the diversity and size of patient datasets would strengthen the generalizability of results while leveraging machine learning tools could support the development of predictive analyses and personalized treatment strategies. These enhancements would bridge the gap between computational modeling and clinical application, improving diagnostic and therapeutic approaches for FAI.

Data availability statement

The original contributions presented in the study are included in the article/supplementary material, further inquiries can be directed to the corresponding author.

Author contributions

FC: Conceptualization, Formal Analysis, Investigation, Methodology, Software, Writing – original draft. CH-S: Conceptualization, Formal Analysis, Investigation, Methodology, Software, Writing – review and editing. OG-E: Conceptualization, Data curation, Formal Analysis, Funding acquisition, Investigation, Methodology, Project administration, Software, Supervision, Validation, Writing – review and editing.

Funding

The author(s) declare that financial support was received for the research and/or publication of this article. This study was supported by Universidad Industrial de Santander (VIE-3716, VIE-3913).

Conflict of interest

The authors declare that the research was conducted in the absence of any commercial or financial relationships that could be construed as a potential conflict of interest.

Generative AI statement

The author(s) declare that no Gen AI was used in the creation of this manuscript.

Publisher's note

References

Aguilera, B., Coaquira, R., and Cantor, E. (2020). Posterior femoroacetabular impact in patients with suspected anterior femoroacetabular impingement evaluated with a 3-dimensional dynamic study. *J. Arthrosc. Jt. Surg.* 7 (3), 127–130. doi:10.1016/j.jajs.2020.08.002

Ardila Parra, S. A., Sánchez Acevedo, H. G., and González Estrada, O. A. (2019). "Evaluation of damage to the lumbar spine vertebrae L5 by finite element analysis," Respuestas, ISSN 0122-820X, ISSN-e 2422-5053, 24, no. 1, pp. 50–55. doi:10.22463/0122820X.1794

Bagce, H., Lynch, T., and Wong, T. (2021). Use of a 3D virtual dynamic hip model to quantify the amount of osteoplasty required in femoroacetabular impingement patients. *Clin. Imaging* 69, 293–300. doi:10.1016/j.clinimag.2020.10.002

Camacho, D., and Mardones, R. (2013). Pinzamiento femoroacetabular: asociación entre el área de sobrecobertura y la zona de delaminación condral acetabular. *Rev. Esp. Cir. Ortop. Traumatol.* 57 (2), 111–116. doi:10.1016/j.recot.2012.11.005

Camilo, A. A., Amorim, P. H. J., Moraes, T. F., Azevedo, F. D. S., and Silva, J. V. L. (2012). "INVESALIUS: Medical image edition," in 1st International Conference on Design and Processes for Medical Devices, 279–282.

Cheng, B., Shrestha, S., and Chou, K. (2016). Stress and deformation evaluations of scanning strategy effect in selective laser melting. *Addit. Manuf.* 12, 240–251. doi:10.1016/j.addma.2016.05.007

Fedorov, A., Beichel, R., Kalpathy-Cramer, J., Finet, J., Fillion-Robin, J. C., Pujol, S., et al. (2012). 3D slicer as an image computing platform for the quantitative imaging network. *Magn. Reson. Imaging* 30 (9), 1323–1341. doi:10.1016/j.mri.2012.05.001

Garcia, S., and Nicot, M. (2007). Segmentación de imágenes médicas con la aplicación de snakes. *Cienc. PC* 4, 12–22.

Grubor, P., Mitković, M., Mitković, M., and Grubor, M. (2019). Comparison of biomechanical stability of osteosynthesis materials in long bone fractures. *Med. Glas.* 16 (1), 88–92. doi:10.17392/985-19

Hellwig, F., Tong, J., and Hussell, J. (2016). Hip joint degeneration due to cam impingement: a finite element analysis. *Comput. Methods Biomech. Biomed. Engin.* 19 (1), 41–48. doi:10.1080/10255842.2014.983490

Hernández-Salazar, C. A., Chamorro, C. E., and González-Estrada, O. A. (2024). Characterization of pig vertebrae under axial compression integrating radiomic techniques and finite element analysis. *Invent* 9, 36. doi:10.3390/INVENTIONS9020036

Jiménez, F., and Cuenca, C. (2015). Síndrome de pinzamiento femoroacetabular en deportista veterano. *Rev. Andal. Med. del Deport.* 8 (4), 171–173. doi:10.1016/j.ramd.2015.04.003

Jorge, J., Simões, F., Pires, E., Rego, P., Tavares, D., Lopes, D., et al. (2014). Finite element simulations of a hip joint with femoroacetabular impingement. *Comput. Methods Biomech. Biomed. Engin.* 17 (11), 1275–1284. doi:10.1080/10255842.2012.744398

Kemp, J., Mosler, A. B., Hart, H., Bizzini, M., Chang, S., Scholes, M. J., et al. (2020). Improving function in people with hip-related pain: a systematic review and meta-analysis of physiotherapist-led interventions for hip-related pain. *Br. J. Sports Med.* 54 (23), 1382–1394. doi:10.1136/bjsports-2019-101690

Lafita, J. (2003). Fisiología y fisiopatología ósea. *An. Sist. Sanit. Navar.* 26 (3), 7–17.

Liberman, U., Weiss, S. R., Bröll, J., Minne, H. W., Quan, H., Bell, N. H., et al. (1995). Effect of oral alendronate on bone mineral density and the incidence of fractures in postmenopausal osteoporosis. *N. Engl. J. Med.* 333 (22), 1437–1444. doi:10.1056/NEJM199511303332201

Longo, U. G., Stelitano, G., Salvatore, G., Candela, V., Di Naro, C., Ambrogioni, L., et al. (2021). "FEA applications for orthopedics: an overview," in *Orthopaedic biomechanics in sports medicine* (Cham: Springer International Publishing), 99–107. doi:10.1007/978-3-030-81549-3_9

Lostado Lorza, R., Somovilla Gomez, F., Corral Bobadilla, M., Íñiguez Macedo, S., Rodríguez San Miguel, A., Fernández Martínez, E., et al. (2021). Comparative analysis of healthy and cam-type femoroacetabular impingement (FAI) human hip joints using the finite element method. *Appl. Sci.* 11 (23), 11101. doi:10.3390/app112311101

Maldonado, J. A., Puentes, D. A., Quintero, I. D., González-Estrada, O. A., and Villegas, D. F. (2023). Image-based numerical analysis for isolated type II SLAP lesions in shoulder abduction and external rotation. *Diagnostics* 13, 1819. doi:10.3390/diagnostics13101819

Maldonado-Moreno, J. F., Martínez-Castañeda, J. S., Beltrán-Malaver, Y. D., Riveros-Pineda, I. C., and Tovar-Hernández, G. D. (2024). Metodología de producción de prótesis de miembro inferior: una revisión exhaustiva. *Rev. UIS Ing.* 23 (2), 167–186. doi:10.18273/REVUIN.V23N2-2024011

Mejía Rodríguez, M., González-Estrada, O. A., and Villegas-Bermúdez, D. F. (2024). Finite element analysis of patient-specific cranial implants under different design parameters for material selection. *Designs* 8 (2), 31. doi:10.3390/designs8020031

Morgado, I., Pérez, A. C., Moguel, M., Pérez, F. J., and Torres, L. M. (2005). Guía de manejo clínico de la artrosis de cadera y rodilla. *Rev. Soc. Española del Dolor* 12 (5), 289–302.

Myers, S., Eijer, H., and Ganz, R. (1999). Anterior femoroacetabular impingement after periacetabular osteotomy. *Clin. Orthop. Relat. Res.* 363, 93–99. doi:10.1097/00003086-199906000-00012

Navarro-Zarza, J. E., Villaseñor-Ovies, P., Vargas, A., Canoso, J. J., Chiapas-Gasca, K., Hernández-Díaz, C., et al. (2012). Clinical anatomy of the pelvis and hip. *Reumatol. Clínica* 8 (Suppl. 2), 33–38. doi:10.1016/j.reuma.2012.10.006

Ng, K., Rouhi, G., Lamontagne, M., and Beaulé, P. (2012). Finite element analysis examining the effects of cam FAI on hip joint mechanical loading using subject-specific geometries during standing and maximum squat. *HSS J.* 8 (3), 206–212. doi:10.1007/s11420-012-9292-x

Noble, P., Dwyer, M., Gobba, M., and Harris, J. (2017). "Functional mechanics of the human hip," in *Hip joint restoration* (New York, NY: Springer), 57–73. doi:10.1007/978-1-4614-0694-5_7

Pegg, E., and Gill, H. (2016). An open source software tool to assign the material properties of bone for ABAQUS finite element simulations. *J. Biomech.* 49 (13), 3116–3121. doi:10.1016/j.jbiomech.2016.07.037

Rachner, T., Khosla, S., and Hofbauer, L. (2011). Osteoporosis: now and the future. *Lancet* 377 (9773), 1276–1287. doi:10.1016/S0140-6736(10)62349-5

Sarassa, C., Carmona, D., Vanegas, D., Restrepo, C., Gomez, L., and Herrera, A. (2021). Pinzamiento femoroacetabular tratado con luxación quirúrgica de la cadera: resultados a corto plazo. *Rev. Esp. Cir. Ortop. Traumatol.* 65 (6), 425–432. doi:10.1016/j.recot.2021.02.002

Scranton, P., McDermott, J., and Rogers, J. (2000). The relationship between chronic ankle instability and variations in mortise anatomy and impingement spurs. *Foot Ankle Int.* 21 (8), 657–664. doi:10.1177/107110070002100805

Shapiro, J. (2021). "Incidence and prevalence of musculoskeletal disease," in *Clinical foundations of musculoskeletal medicine* (Cham: Springer International Publishing), 3–9. doi:10.1007/978-3-030-42894-5_1

Souza, R., and Naves, E. (2019). Numerical evaluation of efforts on the femoral head in a 3D model. *IFMBE Proc.* 70 (1), 323–326. doi:10.1007/978-981-13-2119-1_49

Yong, Q., Hongtao, S., Yueguang, F., Feimeng, L., Yunting, W., and Chana, G. (2018). Three dimensional finite element analysis of the influence of posterior tibial slope on the anterior cruciate ligament and knee joint forward stability. *J. Back Musculoskelet. Rehabil.* 31 (4), 629–636. doi:10.3233/BMR-169703

Yushkevich, P., Piven, J., Hazlett, H. C., Smith, R. G., Ho, S., Gee, J. C., et al. (2006). User-guided 3D active contour segmentation of anatomical structures: significantly improved efficiency and reliability. *Neuroimage* 31 (3), 1116–1128. doi:10.1016/j.neuroimage.2006.01.015

Zhang, Z., Pei, K., Sun, M., Wu, H., Wu, H., Jiang, S., et al. (2022). Tessellated multistable structures integrated with new transition elements and antisymmetric laminates. *Thin-Walled Struct.* 170, 108560. doi:10.1016/j.tws.2021.108560